



Published in final edited form as:

Autism Res. 2018 January ; 11(1): 44–58. doi:10.1002/aur.1853.

Characterization of early communicative behavior in mouse models of Neurofibromatosis type 1

Susan E. Maloney^{1,2,*}, Krystal C. Chandler^{1,2,*}, Corina Anastasaki³, Michael A. Rieger^{1,2}, David H. Gutmann³, and Joseph D. Dougherty^{1,2}

¹Department of Genetics, Washington University School of Medicine, 660 South Euclid Avenue, St. Louis, MO 63110, USA

²Department of Psychiatry, Washington University School of Medicine, 660 South Euclid Avenue, St. Louis, MO 63110, USA

³Department of Neurology, Washington University School of Medicine, 660 South Euclid Avenue, St. Louis, MO 63110, USA

Scientific Abstract

Neurofibromatosis type 1 (NF1) is a monogenic neurodevelopmental disease caused by germline loss-of-function mutations in the *NF1* tumor suppressor gene. Cognitive impairments are observed in approximately 80% of children with this disease, with 45–60% exhibiting autism spectrum disorder (ASD) symptomatology. In light of the high comorbidity rate between ASD and NF1, we assessed early communicative behavior by maternal-separation induced pup ultrasonic vocalizations (USV) and developmental milestones in two distinct *Nf1* genetically-engineered models, one modeling clinical germline heterozygous loss of *Nf1* function (*Nf1*^{+/-} mice), and a second with somatic biallelic *Nf1* inactivation in neuroglial progenitor cells (*Nf1*^{GFAP}CKO mice). We observed altered USV production in both models: *Nf1*^{+/-} mice exhibited both increased USVs across development and alterations in aspects of pitch, while *Nf1*^{GFAP}CKO mice demonstrated a decrease in USVs. Developmental milestones, such as weight, pinnae detachment and eye opening, were not disrupted in either model, indicating the USV deficits were not due to gross developmental delay, and likely reflected more specific alterations in USV circuitry. In this respect, increased whole-brain serotonin was observed in *Nf1*^{+/-} mice, but whole-brain levels of dopamine and its metabolites were unchanged at the age of peak USV disruption, and USV alterations did not correlate with overall level of neurofibromin loss. The early communicative phenotypes reported herein should motivate further studies into the risks mediated by haploinsufficiency and biallelic deletion of *Nf1* across a full battery of ASD-relevant behavioral phenotypes, and a targeted analysis of underlying circuitry disruptions.

Keywords

Neurofibromatosis type 1; NF1; USV; ultrasonic vocalization; communication; mouse; autism

Corresponding Author: Dr. Joseph D. Dougherty, Washington University School of Medicine, Department of Genetics, Campus Box 8232, 660 S. Euclid Avenue, St. Louis, Mo. 63110-1093, (314) 362-0752, jdougherty@genetics.wustl.edu.

*These authors contributed equally to this work.

Introduction

Neurofibromatosis type 1 (NF1) is a common monogenic neurodevelopmental disease with a prevalence of 1 in 3,000 worldwide (Szudek, Birch, Riccardi, Evans, & Friedman, 2000), which is caused by germline loss-of-function mutations of the *NF1* tumor suppressor gene. The *NF1* gene codes for the highly conserved neurofibromin protein. Neurofibromin functions in part as a tumor suppressor by negatively regulating Ras activity. While typically regarded as a tumor predisposition syndrome (Karen Cichowski & Jacks, 2001; Gutmann, 2002; Jett & Friedman, 2010), 80% of children with NF1 exhibit cognitive impairments. These neurocognitive deficits affect academic achievement, attention, executive functioning, visual perception, language, and motor skills (Hyman, Shores, & North, 2005). As such, learning disabilities have been reported in ~50–75% of individuals with NF1 (Jett & Friedman, 2010), and comorbid diagnoses of attention-deficit-hyperactivity disorder (Hyman et al., 2005) and autism spectrum disorder (ASD) are becoming more widely recognized. Indeed, prevalence for ASD among NF1 patients ranges between 15 and 30%, with an additional 30% showing partial ASD symptomatology (Garg, Green, et al., 2013; Garg, Lehtonen, et al., 2013; Walsh et al., 2013). A recent study characterized the quantitative autistic trait burden in a pooled NF1 data set of 531 individuals, and confirmed that the diversity of mutations that give rise to NF1 may function as a quantitative trait loci for ASD (Morris et al., 2016). ASD is a neurodevelopmental disorder characterized by social and communication interaction deficits, and repetitive patterns of behavior (American Psychiatric Association, 2013). While the mechanistic underpinnings of the tumor-related clinical features of NF1 are fairly well understood, less is known about the role of *NF1* gene mutations in ASD comorbidity.

Murine genetically-engineered models (GEM) with mutations in the homologue of the human *NF1* gene (*Nf1*) recapitulate many aspects of the disease, including optic nerve gliomas, neurofibromas, and skeletal abnormalities. They also provide unique opportunities to study the disruption of behavioral circuits in the context of impaired *Nf1* function (Atit, Mitchell, Nguyen, Warshawsky, & Ratner, 2000; K. Cichowski et al., 1999; Zhu, Ghosh, Charnay, Burns, & Parada, 2002). *Nf1* heterozygous mutant (*Nf1*^{+/-}) mice model a single germline loss-of-function mutation (haploinsufficiency), genetically analogous to individuals with NF1 (germline *NF1* gene mutation). Previous behavioral characterization of adult *Nf1*^{+/-} mice has shown impaired spatial learning and memory in the Morris water maze with LTP deficiencies that are Ras-dependent and social recognition deficits related to the MAP kinase signaling pathway and altered prefrontal cortex volume (Costa et al., 2002; Molosh et al., 2014; Petrella et al., 2016). Additionally, some of these behavioral deficits (exploratory behaviors, learning/memory) were linked to altered dopamine levels in the hippocampus (Anastasaki, Woo, Messiaen, & Gutmann, 2015). Spatial and contextual learning and memory deficits displayed by *Nf1*^{+/-} mice in the Morris water maze and fear conditioning, respectively, were also linked to Anaplastic Lymphoma Kinase activity (Weiss, Weber, Torres, Marzulla, & Raber, 2017; Weiss, Weber, Marzulla, & Raber, n.d.). *Nf1*^{+/-} mice also demonstrated normal associative learning and olfaction, and did not display anxiety- or depression-related behaviors in the elevated plus maze and light/dark box or forced swim assay, respectively (Molosh et al., 2014; Silva et al., 1997). Germline haploinsufficient mice

with a somatic biallelic deletion in neuroglial progenitor cells of the brain (*Nf1*^{+/-GFAP}CKO mice), were originally developed to specifically model the somatic loss of *Nf1* thought to underlie development of optic pathway gliomas (Bajenaru et al., 2003). In addition to optic gliomas and visual acuity deficits, these mice showed attention, spatial and associative memory deficits, hypoactivity, and altered emotionality (Brown et al., 2010; Diggs-Andrews et al., 2013; Wozniak et al., 2013). The behavioral disruptions in these mice were linked to altered dopamine levels in the striatum, and were sexually dimorphic (Diggs-Andrews et al., 2014). Lastly, mice harboring only this, somatic, biallelic deletion of *Nf1* in neuroglial progenitor cells in the absence of germline heterozygosity (*Nf1*^{GFAP}CKO mice) also exhibited memory deficits in the Morris water maze that were linked to altered hippocampal DA levels (Anastasaki et al., 2015), suggesting a second, somatic mutation of the remaining allele can disrupt brain function.

Importantly, none of the existing *Nf1* mouse models have been assessed for early communicative deficits through ultrasonic vocalizations that might provide insights into brain circuit disruptions relevant to ASD and language impairments. Ultrasonic vocalizations (USVs) are whistle-like sounds emitted by rodents with frequencies from 30 kHz to 150 kHz, and are a form of communication as pups will emit USVs in response to maternal separation, eliciting a search and retrieval response from the mother (D'Amato, Scalera, Sarli, & Moles, 2005; G. Ehret, 1987, 1992; Günter Ehret & Haack, 1982; Hahn & Lavooy, 2005; Smith, 1976; Wöhr et al., 2008). Specifically, in playback experiments, lactating females have been shown to respond rapidly with searching behavior to pup isolation call (Haack, Markl, & Ehret, 1983; Sewell, 1970). In addition, these behaviors are dependent on acoustic call features, such as duration and frequency, indicating these features have communicative value (Günter Ehret & Haack, 1982; Smith, 1976; Wöhr et al., 2008). As production of this behavior has a distinct developmental trajectory, it can be used to study both early communication and neurobehavioral development in infant rodents (Igor Branchi, Santucci, & Alleva, 2001; Moy, Nadler, Magnuson, & Crawley, 2006). Previous studies investigating USV production in other mouse models of ASD have found deviations from baseline vocalization rates (Dougherty et al., 2013; Scattoni, Gandhi, Ricceri, & Crawley, 2008; Wöhr, 2014), and this has been interpreted as a sign of communication impairment or affective disturbance. Recent reviews of a large number of USV studies involving ASD models report the majority demonstrate a phenotype (Lai et al., 2014; Michetti, Ricceri, & Scattoni, 2012), with a variety of specific alterations of USV features including fewer calls, shorter call duration, increased number of calls, and dam-specific effects.

Based on the prevalence of ASD in children with NF1 and the ability to model these neurobehavioral deficits in mice, we sought to better understand the consequence of *Nf1* disruption on these early communicative behaviors. In this report, we investigated two *Nf1* mutant mouse lines during the early postnatal period. Both germline deletion (*Nf1*^{+/-}) and a biallelic somatic mutation during neural development (*Nf1*^{GFAP}CKO mice) led to alterations in these behaviors in the absence of gross developmental delay.

Methods

Animals

All protocols involving animals were approved by the Animal Studies Committee of Washington University. The animal colony room lighting was a 12:12 h light/dark cycle; room temperature (~20°C–22°C) and relative humidity (50%) were controlled automatically. Standard laboratory chow and water were available on a continuous basis. Two mouse models containing mutations within the *Nf1* gene were used in this study (Figure 1A). In this manuscript, we have used the accepted *Nf1* legacy numbering system (Barron & Lou, 2012). For example, legacy ‘exon 31’ is exon 39 in a consecutive numbering based on the UCSC Genome Browser alignment of reference sequence NM_010897. We included UCSC exon numbering in parentheses. Homozygous germline *Nf1* mutants are embryonically lethal in rodent models, and therefore not represented in human populations (Gutmann & Giovannini, 2002). We therefore examined heterozygous mutant mice and conditional deletion mice. Generation of *Nf1*^{+/-} mice (Brannan et al., 1994; Costa et al., 2002; Jacks et al., 1994) and *Nf1*^{GFAPCKO} mice (Bajenaru et al., 2002; Zhu et al., 2001) have been described previously. Briefly, the loss-of-function allele in *Nf1*^{+/-} mice was generated by insertion of a neomycin cassette in place of the first 126 nucleotides of exon 31 (39), including the exon 31 splice acceptor sequence and approximately 2 kilobases of intron 30 (Figure 1A). This results in a lack of stable neurofibromin production from this allele (Brannan et al., 1994; Jacks et al., 1994). This exon is a focus of interest because several missense and nonsense mutations have been observed in this exon in people with NF1 (Ainsworth, Rodenhiser, & Costa, 1993; Cawthon et al., 1990; Jacks et al., 1994). We also employed Cre-loxP to model a somatic mutation during neural development, leading to loss of both *Nf1* alleles in neuroglial progenitor cells (Anastasaki et al., 2015; Bajenaru et al., 2002) and their progeny, leaving all other cells with two functional copies of the *Nf1* gene (*Nf1*^{GFAPCKO} mice). *Nf1*^{FF} mice contain a loxP site with a neomycin cassette within intron 30 and a second loxP site within intron 32, thereby flanking exons 31 (39) and 32 (40) by loxP sites. Cre recombinase under the human glial fibrillary acidic protein (hGFAP) promoter excises this portion of the gene resulting in a premature stop codon and biallelic loss-of-function in neuroglial progenitor cells (*Nf1*^{GFAPCKO}) (Brown et al., 2010; Zhu et al., 2001), and their neuronal and glial progeny (Figure 1A). For *Nf1*^{+/-} mice, wild type littermates were used in parallel as controls, and Cre negative *Nf1*^{FF} mice served as controls for the conditional deletion line. All animals were maintained on a C57BL/6J background.

Nf1^{+/-} males were crossed to C57BL/6J wild type females to produce 36 *Nf1*^{+/-} mice and 36 *Nf1*^{+/+} control littermates, representing a total of 14 independent litters, for behavioral analysis of germline mutants. For the biallelic somatic mutant experiments, *Nf1*^{FF} females and *Nf1*^{GFAPCKO} males were crossed to generate 38 *Nf1*^{GFAPCKO} mice and 35 litter-matched *Nf1*^{FF} controls from a total of 10 independent litters. (Table 1). Males and females were included for each line to allow assessment of any sex differences. Wild type females were used as dams to control for any maternal behavior changes that might result from *Nf1* loss in the dam. A power analysis to determine the appropriate sample size for a repeated measure ANOVA with main and interaction effects using a large effect size of $f = .40$ and 80% power indicates that a total sample size of 34 animals is required to reject the null

hypothesis at the .05 alpha level (Faul, Erdfelder, Lang, & Buchner, 2007). Our total samples of 72 and 73 for *Nf1*^{+/-} and *Nf1*^{GFAPCKO} experiments are thus adequately powered.

Immunoblotting

Whole brains were dissected and snap-frozen from postnatal day (P)21 mice. The tissue was homogenized in 1 mL lysis buffer (20mM Tris pH7.5, 10mM EGTA, 40mM b-glycerophosphate, 1% Igepal Ca 630, 2.5mM MgCl₂, 2mM sodium orthovanadate; Sigma) supplemented with Aprotinin (1:1000) (Sigma), Leupeptin (1:100) (Sigma) and PMSF (1:100) (Sigma) by sonication. Remaining debris was removed by centrifugation at 16,168rcf at 4°C. The supernatant samples were collected and protein concentration was determined by BCA assay. Fifty to seventy µg of total protein was loaded on a 8% polyacrylamide gel for the detection of neurofibromin and 5µg of total protein were loaded on 10% polyacrylamide gels for the detection of α-tubulin (loading control). Gels were analyzed by PAGE electrophoresis and transferred on a PVDF membrane. Western blotting was performed as previously described (Anastasaki et al., 2015). Briefly, the gels were blocked in 5% milk in TBS-T (1%), probed with either neurofibromin sc-67 (Santa Cruz Biotechnology; 1:200) or α-tubulin (Life Sciences; 1:60,000) primary antibodies followed by appropriate secondary horseradish peroxidase-conjugated antibodies (Sigma-Aldrich). Neurofibromin and α-tubulin were detected by ECL chemiluminescence (Pierce ECL2 Western Blotting Substrate; ThermoFisher Scientific) in a UVP chemidock imaging system. Protein intensity was quantified using densitometry using ImageJ (NIH, USA) software to determine relative amounts of protein in each lane and neurofibromin levels were normalized to total α-tubulin levels as an internal loading control. We report neurofibromin levels as the normalized ratio of each animal's detected neurofibromin expression/α-tubulin (housekeeping gene) expression, in order to account for the slight variation in total protein loaded in each well, as depicted by the small differences in α-tubulin expression. Analyses of α-tubulin levels between genotypes showed comparable levels for *Nf1* mutants and control littermates. The histograms graphed (Figure 1) represent the mean of the neurofibromin/α-tubulin ratio of all animals analyzed in each genotype compared to their respective littermate controls. These values were calculated as follows: Following initial neurofibromin/α-tubulin normalization of all animals in each cohort, we averaged the neurofibromin/α-tubulin ratio of all control (CTL) animals in that cohort and set that as the control reference point [AVG neurofibromin_{CTL}/α-tubulin_{CTL}]. We then calculated the neurofibromin/α-tubulin ratio fold-change differences between every animal in the cohort and the control reference point as follows: (neurofibromin_{animal}/α-tubulin_{animal})/[average (neurofibromin_{CTL}/α-tubulin_{CTL})]. For comparisons between control and *Nf1*^{+/-} animals, a total of n=8 female animals/genotype; n=9 male animals/genotype were used. For comparisons between control and *Nf1*^{GFAPCKO} animals, a total of n=4 female animals/genotype; n=8 male animals/genotype were used.

Ultrasonic vocalization recording and analysis

USV recording occurred on P5, 7, and 9. Parents were removed from the home cage and placed into a clean standard mouse cage for the duration of testing. Pups in the home cage were placed into a warming box for at least 10 minutes prior to the start of testing to control temperature. Skin surface temperature was monitored via a noncontact HDE Infrared

Thermometer during recordings to ensure consistent temperatures. For recording, pups were individually removed from the home cage and placed into an empty standard mouse cage inside a sound-attenuating chamber. USVs were obtained using an Avisoft UltraSoundGate CM16 microphone, Avisoft UltraSoundGate 416H amplifier, and Avisoft Recorder software (gain = 3 dB, 16 bits, sampling rate = 250 kHz). Pups were recorded for 3 min, after which they were weighed and returned to their home cages inside the warming box. Tissue from a toe was also collected at this time on P5 for genotyping. Frequency sonograms were prepared from recordings in MATLAB (frequency range = 25 kHz to 120 kHz, FFT size = 512, overlap = 50%, time resolution = 1.024 ms, frequency resolution = 488.2 Hz), and individual syllables and other spectral features were identified and counted from the sonograms according to a previously published method (Holy & Guo, 2005; Rieger & Dougherty, 2016).

Developmental milestones and general health examination

Mice were evaluated at several time points for achievement of physical and behavioral milestones of development. A visual check for the presence of detached pinnae was done on P5, and eye opening on P14. Weight was measured on P5, 7, 9 and 14, concurrent with USV recordings and righting reflex testing. To assess surface righting reflex on P14, each mouse was placed in a 50 ml conical containing a lid with a hole. When the belly of the mouse was facing down, the conical was quickly turned 180 degrees in a smooth motion placing the mouse on its back. The time for the mouse to right itself with all 4 paws underneath its belly was recorded up to 60 sec. Each mouse received 3 trials, which were averaged for analysis.

Monoamine analysis

High pressure liquid chromatography (HPLC) was used to quantify levels of dopamine (DA) and serotonin (5-HT), and their metabolites 3,4-Dihydroxyphenylacetic acid (DOPAC), homovanillic acid (HVA), and 5-hydroxyindoleacetic acid (5-HIAA) in *Nfl* mutants and controls as previously described (Dearborn et al., 2015). Brains were collected from P7 (*Nfl*^{GFAPCKO} and *Nfl*^{FF} littermates) or P9 (*Nfl*^{+/-} and *Nfl*^{+/+} littermates) mice. Mouse pups were sacrificed via rapid decapitation and the brains were rapidly removed. For monoamine analysis, the brain was homogenized in 2- or 2.5-fold (weight: volume) ice-cold PCA buffer (0.1 N perchloric acid, 0.2 mM sodium metabisulfite) in a glass Teflon homogenizer. The homogenized tissue centrifuged at 10,000 RCF for 15 min at 4 °C. The supernatant was stored at -80 °C. HPLC was performed using an ESA Coulochem III electrochemical detector (Bedford, MA) on a MD-150 × 3.2 mm column with MD-TM HPLC buffer (75 mM sodium dihydrogen phosphate, monohydrate; 1.7 mM 1-octanesulfonic acid, sodium salt; 100 µL/L triethylamine; 25 µM EDTA-tetrasodium salt, tetrahydrate; 10% acetonitrile; pH 3.0). The samples were diluted with MDTM HPLC buffer and filtered through a 0.22 µm syringe filter to remove any fine particulates. 100 µL was injected onto the HPLC and eluted with MD-TM mobile phase at a rate of 0.6 mL/min. Concentrations of DA, 5-HT, DOPAC, HVA and 5-HIAA in the whole-brain samples were obtained by comparing to a series of monoamine standards. The levels of the neurochemicals were normalized to tissue weights.

Statistical analyses

All statistical analyses were performed using the IBM SPSS Statistic software (v.23) and MATLAB software. Independent t-tests, factorial ANOVAs, included repeated measures (rm) ANOVAs, and mixed-model analyses were used where appropriate. The appropriate correction, Huynh-Feldt or Greenhouse-Geisser, was applied to violations of the sphericity assumption within rmANOVAs. With a statistically significant interaction between main factors, simple main effects were calculated post-hoc to provide clarification of statistically significant between-genotype and within-genotype differences. All data were analyzed for genotype and sex effects, and genotype interactions with sex are reported where significant. Multiple comparisons were Bonferroni adjusted. Probability value for all analyses was $p < .05$.

Results

Neurofibromin levels are differentially reduced by heterozygosity and biallelic deletion of the *Nf1* gene

To establish the impact of *Nf1* mutations on behavioral and physiological development in pups, we employed two distinct *Nf1* GEM mouse lines: heterozygous mutants and conditional biallelic deletion mutants (Figure 1A). Each line has been shown to have reduced neurofibromin expression (Brannan et al., 1994; Jacks et al., 1994). Indeed, using immunoblotting, we observed a 52% reduction in neurofibromin levels in *Nf1*^{+/-} mice relative to their control littermates (Figure 1B). Reduced neurofibromin was observed in both female and male brains, 55% and 50% of controls, respectively. *Nf1*^{GFAPCKO} mice have a 77% reduction (80% in females and 74% in males) in neurofibromin levels in the brain compared to *Nf1*^{FF} littermates (Figure 1C). Consistent with previous findings (Anastasaki et al., 2015), these results demonstrate reduced brain neurofibromin levels relative to control littermates following heterozygosity or biallelic deletion of *Nf1*.

Nf1 heterozygosity alters early communicative behavior

Nf1 heterozygous mutant mice were examined for USV production and developmental milestones during the first two weeks of postnatal life. *Nf1*^{+/-} mice exhibited an increase in USV production when isolated from the dam compared to control littermates overall, $F(1,68) = 5.737$, $p = .019$ (Figure 2A). Furthermore, a trend was observed for the interaction between sex and *Nf1* mutation, $F(1,68) = 3.573$, $p = .063$, for male *Nf1*^{+/-} mice produced more USV calls than male control littermates, $F(1,68) = 7.669$, $p = .007$, and female *Nf1*^{+/-} mice, $F(1,68) = 4.611$, $p = .035$ (Figure 2B). Examination of the USV call number at each age revealed *Nf1*^{+/-} mice displayed a trend towards more USVs at P7, $F(1,204) = 3.691$, $p = .056$, and significantly more on P9, $F(1,204) = 6.570$, $p = .011$ (Figure 2C). Both *Nf1*^{+/-} and control mice demonstrated the expected change in call numbers with age, $F(2,67) = 18.811 - 34.476$, $p < .000005$ (Figure 2C). While control mice showed a peak in call numbers by P7 ($p < .05$, 95% CI [48.59, 158.58]), which was unchanged at P9, *Nf1*^{+/-} mice showed further increase by P9 (P7 $p < .05$, 95% CI [88.45, 202.23] and P9 $p < .05$, 95% CI [-6.865, 137.44]).

Examination of the spectral features of the USV calls produced during the maternal separation assay revealed changes to the frequency features of the calls produced by *Nf1*^{+/-} mice. While no differences were observed between mutants and controls for features, such as duration of call and fraction of calls with pitch jumps (Figure 3A, B), USVs produced by *Nf1*^{+/-} mice were lower in mean frequency compared to littermate controls, $F(1,67.833) = 5.429$, $p = .023$ (Figure 3C). This change was most pronounced at P7, $F(1,150.915) = 5.647$, $p = .019$. Both *Nf1*^{+/-} mice and controls increased mean frequency from P5 to P9, ($p < .05$, 95% CI [342.62, 6572.13] and [241.1, 6651.33], respectively). Mice produce two call types: flat calls that do not contain a pitch jump and dynamic calls that contain a pitch jump. The pitch range for dynamic calls was narrower for *Nf1*^{+/-} mice compared to controls, $F(1,168.563) = 5.675$, $p = .018$, particularly at P9, $F(1,65) = 5.096$, $p = .027$ (Figure 3D). The pitch range of both controls and mutants increased with age, $F(2,118.76) = 4.473$, $p = .013$ and $F(2,121.503) = 3.268$, $p = .041$, respectively. Examination of the pitch range of flat calls revealed a genotype x sex x age interaction, $F(7,129.517) = 2.719$, $p = .012$, due to a narrower pitch range by female *Nf1*^{+/-} mice at P7, $F(1,116.846) = 6.158$, $p = .015$ and P9, $F(1,115.322) = 4.692$, $p = .032$, respectively (Figure 3E). Female *Nf1*^{+/-} mice were also different from male *Nf1*^{+/-} mice at P9, $F(1,115.322) = 5.276$, $p = .023$. Body temperature of the pup is known to influence USV production: the colder a mouse, the more calls produced (I. Branchi, Santucci, Vitale, & Alleva, 1998). Thus, temperature of each pup was recorded immediately prior to placement in the USV recording chamber. We did not observe any differences in temperature between mutants and controls, indicating the differences in USV production were not secondary to thermoregulation differences (data not shown). These data indicate this germline single copy loss-of-function mutation altered communicative behaviors in mouse pups.

As a measure of general health, we recorded the weight of all mice on days we also conducted a developmental assessment (P5, P7, P9 and P14). All mice exhibited an increase in weight across developmental time points, as expected, $F(3,183) = 423.074$, $p < .000005$ (Supplemental Figure 1A). No difference in weight was observed between *Nf1*^{+/-} and control littermates at any age. Assessment of developmental milestones revealed no effect of germline *Nf1* mutation on pinnae detachment by P5 or eye opening at P14 (data not shown). To assess early gross locomotor abilities and to evaluate general body strength, we tested all mice in this cohort for latency to exhibit a righting reflex at P14. We observed no difference between the *Nf1*^{+/-} and control littermates for time to right (Supplemental Figure 1B).

Robust early communicative deficits in mice result from somatic biallelic loss of *Nf1* during development

Mice with *Nf1* biallelic deletion in neuroglial progenitor cells (*Nf1*^{GFAP}CKO mice) were examined for USV and developmental milestones during the first two postnatal weeks. The hGfap-Cre mouse strain used for these experiments is confirmed to delete *Nf1* from neuroglial progenitors during late embryonic development (~E15.5) (Anastasaki et al., 2015; Bajenaru et al., 2002). In this line, no effect of sex was observed for any variable examined; therefore, we collapsed the data by sex for all analyses reported. Biallelic deletion of *Nf1* in neuroglial progenitors resulted in altered of USV call production when isolated from the dam on P5, P7, and P9. *Nf1*^{GFAP}CKO mice produced fewer USV calls during development

relative to their control littermates, $F(1,71) = 5.963$, $p = .017$ (Figure 4A). Examination of the USVs at each age (Figure 4B) revealed the greatest difference in call production on P7, $F(1,213) = 7.660$, $p = .006$. A large decrease in call rate produced by $Nf1^{GFAPCKO}$ mice was also observed on P5, $F(1,213) = 3.048$, $p = .082$, although the difference did not reach statistical significance. All mice increased call production with age, $F(2,142) = 8.742$, $p = .000$, as expected. Within each genotype, control mice showed an increase in calls, $F(2,70) = 5.670$, $p = .005$, from P5 to P7 ($p < .05$, 95% CI [20.45, 156.35]) and P9, although the difference from P9 did not reach statistical significance ($p < .1$, 95% CI [-2.02, 142.420]). $Nf1^{GFAPCKO}$ littermates also demonstrated an increase in USVs, $F(2,70) = 4.735$, $p = .012$, only from P5 to P9 ($p < .05$, 95% CI [16.53, 155.15]). Examination of the spectral features of the USV calls produced during maternal separation assay did not reveal any differences between genotypes (Figure 5), suggesting that $Nf1^{GFAPCKO}$ mice are able to produce calls similar to their control littermates. Spectral features cannot be assessed if < 10 calls are produced, and a significant portion of the $Nf1^{GFAPCKO}$ mice produced < 10 calls per session (Table 2). Since different mice produced such low rate of calls from day to day, the assessments of spectral features in $Nf1^{GFAPCKO}$ mice are likely accurate. Overall, the USV phenotype among $Nf1^{GFAPCKO}$ mice indicates that complete somatic loss of neurofibromin in a large population of brain cells decreases this early communicative behavior in mouse pups.

As a measure of general health, we also analyzed weight differences on P5, P7, P9 and P14. All mice exhibited an expected increase in weight across developmental time points. Both experimental, $F(3,69) = 445.821$, $p = .000$, and control, $F(3,69) = 430.266$, $p = .000$, animals gained weight at each age (Supplemental Figure 1C). A significant interaction between genotype and age, $F(1.197,84.980) = 5.639$, $p = .015$, was driven by a decrease in weight of the $Nf1^{GFAPCKO}$ mice at P14 compared to littermate controls, $F(1,284) = 5.965$, $p = .015$. Assessment of developmental milestones revealed no effect of genotype on pinnae detachment by P5 or eye opening at P14 (data not shown). We also observed no difference between $Nf1^{GFAPCKO}$ mice and their control littermates for time to exhibit righting reflex at P14 (Supplemental Figure 1D).

Whole-brain serotonin levels altered by *Nf1* loss-of-function mutation

Monoaminergic system dysfunction has been previously demonstrated in NF1 and other ASD-related mutants. We previously reported altered whole-brain 5-HT levels in a mutant model demonstrating robust decreases in postnatal USV production, as well as in other ASD-related behavioral deficits (Dougherty et al., 2013). We also demonstrated behavioral disruptions in adult $Nf1^{+/-GFAPCKO}$ mice were due to altered DA activity (Brown et al., 2010; Diggs-Andrews et al., 2013; Wozniak et al., 2013), and linked memory deficits in $Nf1^{+/-GFAPCKO}$ and $Nf1^{GFAPCKO}$ mice to altered DA levels in the hippocampus. Since specific regions mediating pup USV are unknown, we measured whole-brain levels of 5-HT, DA and their metabolites in *Nf1* mutants and littermate controls to determine if USV production may be related to overall monoamine levels. We examined brains at the postnatal age at which the most robust USV alteration was observed in each line. Increased levels of whole-brain 5-HT were present in $Nf1^{+/-}$ mice (Table 3). $Nf1^{+/-}$ brains had greater levels of 5-HT, $t(4) = 3.465$, $p = .026$, compared to $Nf1^{+/+}$ (wild-type) control brains. Higher levels of

5-HT and 5-HIAA were observed in *Nfl*^{GFAPCKO} brains, $t(5) = 2.355$, $p = .065$ and $t(5) = 2.145$, $p = .085$, respectively, although this did not reach statistical significance. We did not observe altered levels of whole-brain DA or its metabolites, DOPAC and HVA, in P7 *Nfl*^{GFAPCKO} mice or in P9 *Nfl*^{+/-} mice compared to control littermates (Table 3). It is possible that the USV disruptions in *Nfl*^{+/-} mice are linked to 5-HT alterations, but future experiments will be required to prove causality. While a robust overall change in DA levels was not present, our results do not exclude the possibility that the USV phenotype may be linked to monoamine alterations in specific brain regions.

Discussion

The high comorbidity rate between NF1 and ASD warrants relevant behavioral testing in the *Nfl* mouse models to fully understand the expressivity of *Nfl* mutations on ASD phenotypes. In the current study, we demonstrate, for the first time, early neurobehavioral disruptions relevant to early social communicative behavior in two independently-generated murine *Nfl* mouse models. Specifically, *Nfl*^{+/-} mice exhibit an increase in USV calls, with altered aspects of frequency pitch during postnatal separation from the dam and litter. In contrast, somatic biallelic *Nfl* deletion in *Nfl*^{GFAPCKO} mice results in a decrease in USV call production at early postnatal ages. USVs are considered a strongly conserved affective and communicative display that elicits maternal search and retrieval responses, nursing, and caretaking, and is used in the rodent literature to model early communicative deficits (Günter Ehret & Haack, 1982; Haack et al., 1983; Hofer, Shair, & Brunelli, 2002; Sewell, 1970; Smith, 1976). USV production due to maternal isolation in the C57BL/6J mouse pup normally peaks just after P7, disappearing completely by P14 (Rieger & Dougherty, 2016). The USV production of *Nfl*^{GFAPCKO} mice suggests a developmental neurobehavioral delay, as call number is reduced at younger ages, P5 and P7, but became equivalent to control littermates by P9. Furthermore, while controls showed an increase in call rate by P7, *Nfl*^{GFAPCKO} mice did not exhibit a significant increase until P9. The age-related neurobehavioral profile of USVs in the *Nfl*^{+/-} mice was also altered as they continued to increase calls until P9, different from their littermate controls. The increased USVs observed in this line at later postnatal ages demonstrate abnormal decline of the behavior and, therefore, abnormal neurobehavioral maturation of the pups. This finding suggests possible developmental delay of early social communicative behavior. Pup USV calls have been related to anxiety levels. Specifically, high-anxiety mouse lines produce more such calls than low-anxiety lines (Krömer et al., 2005). It is possible the increased calls in the *Nfl*^{+/-} pups result from an increased anxiety state. However, previous investigations have not found increased anxiety levels in emotionality tasks like the light-dark box or elevated plus maze in *Nfl*^{+/-} mice (Molosh et al., 2014). It is important to note that our USV findings do not result from *gross* developmental delay or altered maternal behavior. All mice were comparable for achievement of physical milestones, such as pinnae detachment, eye opening and weight, as well as the righting reflex. Previous studies showed USV alterations resulting from dam genotypes (van Velzen & Toth, 2010; Weller et al., 2003; Young, Schenk, Yang, Jan, & Jan, 2010). Only control females were used as dams in our study, therefore, maternal *Nfl* genotype did not influence pup USV calls via change to maternal behavior.

Deviations from baseline vocalization rates have been reported previously in other mouse models of syndromic ASD, such as those for Fragile-X, Rett, and Timothy syndromes. *Fmr1* knockout mice, a model for Fragile-X syndrome, emitted more calls, specifically those with frequency jumps, that were longer in duration than those emitted by wild type controls (Lai et al., 2014). In a mouse model for Rett syndrome, the *Mecp2-308* mutant, heterozygous pups emitted significantly fewer calls than their wild-type counterparts. However, it should be noted that this decrease in calls may be related to poor respiratory function in this model (De Filippis, Ricceri, & Laviola, 2010). Shorter call duration was seen in a mouse model of Timothy syndrome, *TS2-neo* heterozygous mice, without a differences in call number compared to wild-type controls (Bader et al., 2011). A large number of other ASD models also show either increases or decreases in USV production (Michetti et al., 2012). Thus, our results are consistent with those observed in other murine models of syndromic ASD, and indicate heterogeneity in disruptions of early social communicative behaviors across genetic ASD mouse models. The distinct phenotypes we observed in *Nfl*^{+/-} and *Nfl*^{GFAPCKO} mice, both the increase and decrease in USVs, respectively, may reflect the heterogeneity of early communicative disruptions that result from subtle, but distinct, differences in loss-of-function mutations, and suggest the ability of somatic mutations to alter final phenotype. The mechanism underlying the differences in phenotype in *Nfl*^{+/-} and *Nfl*^{GFAPCKO} mice is unclear. To understand the etiology of the distinct USV phenotypes reported here, further studies are needed to map the brain circuitry of pup USV behavior and how that circuitry is disrupted in each *Nfl*^{+/-} and *Nfl*^{GFAPCKO} mice. It is possible the 5-HT levels create a distinct effect in each mouse line, but which may only be observable at the circuit or structure level. A direct circuit has been identified from the layer V pyramidal projection neurons in the primary motor cortex to the nucleus ambiguus that is active during adult mouse USV production, with activation of immediate early genes in the primary and secondary motor cortices and anterodorsal striatum (Arriaga, Zhou, & Jarvis, 2012), yet studies are needed to identify areas active during isolation-induced pup USV. Future work investigating the actively translated transcriptomes in these areas of the *Nfl*^{+/-} and *Nfl*^{GFAPCKO} pup brain may help elucidate the differential molecular mechanisms of enhanced versus reduced USV production, respectively, in these mice. Indeed, mapping the circuitry of pup isolation calls will enable the identification of convergent and divergent cellular and circuitry-level mechanisms of USV disruptions in differing monogenic forms of ASD and will help us understand the heterogeneity of this behavior.

While the neurochemical defects responsible for the observed abnormal vocalizations have not been established, our data suggest that change in 5-HT levels may be sufficient, but not necessary, to alter USV production in *Nfl*-mutant pups, however, further research in this area is needed. Alterations in the serotonergic system have been repeatedly shown to influence USV production (for review, see (Wöhr, van Gaalen, & Schwarting, 2015)). Of particular relevance, we previously reported whole-brain reduction in 5-HT in *Cellf6* homozygous mutant mice, which also display robust decreases in pup USVs (Dougherty et al., 2013). The increase in 5-HT levels observed in *Nfl*^{+/-} pups may be linked to this increase in USVs. Further studies are needed to understand the possible direct correlation between 5-HT levels and USV call rate in the *Nfl*^{+/-} mouse pup, as well as the mechanism underlying the higher 5-HT levels in *Nfl*^{+/-} mice.

We did not observe large effects of sex on neurobehavioral development in the *Nf1* models employed in this study. Among male *Nf1*^{+/-} mice, a trend was observed towards increased calls over male controls, indicating the overall effect may be driven by differences between males. Our *Nf1*^{+/-} breedings produced slightly more females than males (Table 1), therefore this study may be underpowered to observe a significant sex effect in this line. In addition, we observed sexual dimorphism in pitch range of flat calls produced by *Nf1*^{+/-} mice. Specifically, female *Nf1*^{+/-} mice produced flat calls in a narrower pitch range compared to female controls. It is possible that complete germline haploinsufficiency for *Nf1* differentially affects aspects of USV in males and females. Further investigation will be required to better understand whether sex is a biological factor underlying early communicative behaviors in *Nf1* mutant mice.

The findings in this current study highlight an interesting phenomenon surrounding early communicative behaviors in *Nf1* mutant mice. Specific USV disruptions can be caused by germline *Nf1* haploinsufficiency in all cells and by developmental somatic biallelic *Nf1* loss within a large, but incomplete, population of brain cells. Clinically, somatic biallelic inactivation of *NF1* results in formation of tumors such as pilocytic astrocytomas, malignant nerve sheath tumors, neurofibromas, café-au-lait macules and glomus tumors (Gutmann et al., 2013; Jouhilahti, Peltonen, Heape, & Peltonen, 2011; Spyk, Thomas, Cooper, & Upadhyaya, 2011). It is possible this somatic loss of heterozygosity is not restricted to tumorigenesis and, when it occurs in cell populations underlying behavioral regulation, disrupted behavioral phenotypes emerge. In this regard, biallelic *Nf1* loss in dopaminergic neurons was required to demonstrate a defect in spatial learning and memory, which was not observed in mice with heterozygous *Nf1* inactivation (Anastasaki et al., 2015). Additional evidence from clinical genetic work supports the hypothesis that somatic mutation within only a small subset of brain cells can result in profound phenotypes, as deleterious somatic mutations have been found in ASD cases in brain-region-specific patterns (D’Gama et al., 2015). Moreover, other data suggest that somatic mutations which result in a clear disorder may be detected in only 10% of cells (Jamuar et al., 2014). An interesting suggestion is the variation in expressivity of ASD symptoms in NF1 patients may be due to region-specific somatic *NF1* mutations or somatic mutations in other genes that then interact with the present germline *NF1* mutation.

While the maternal isolation pup USV assay is a standard assay for early social communicative and affective behavior in mouse models of ASD, it does not capture the entire spectrum of clinical ASD conferred by a candidate gene mutation. The early communicative phenotypes reported herein should therefore motivate further studies into the risk mediated by *Nf1* mutation across a full battery of ASD-relevant behavioral phenotypes examining both social and communicative interactions, as well as repetitive and restricted patterns of behaviors in these models.

Supplementary Material

Refer to Web version on PubMed Central for supplementary material.

Acknowledgments

The authors would like to thank Steve Harmon, Karen O'Malley, and Courtney Corman for their assistance in HPLC and mouse husbandry. This work was supported by the W.M. Keck Foundation (SEM), a NARSAD Independent Investigator grant from the Brain and Behavior Research Foundation (JDD), the McDonnell Centers for System Neuroscience (JDD), the NHGRI (R25HG006687 training grant; KCC) and the NIH (U01MH10913301 and 1R01NS102272-01; JDD). DHG is supported by a Research Program Award from the National Institute of Neurological Disorders and Stroke (1-R35-NS097211-01). Authors do not have conflicts of interests to declare.

References

- Ainsworth PJ, Rodenhiser DI, Costa MT. Identification and characterization of sporadic and inherited mutations in exon 31 of the neurofibromatosis (NF1) gene. *Human Genetics*. 1993; 91(2):151–156. [PubMed: 8385067]
- American Psychiatric Association. Diagnostic and statistical manual of mental disorders: DSM-5. 2013. Retrieved from <http://dsm.psychiatryonline.org/book.aspx?bookid=556>
- Anastasaki C, Woo AS, Messiaen LM, Gutmann DH. Elucidating the impact of neurofibromatosis-1 germline mutations on neurofibromin function and dopamine-based learning. *Human Molecular Genetics*. 2015; 24(12):3518–3528. <https://doi.org/10.1093/hmg/ddv103>. [PubMed: 25788518]
- Arriaga G, Zhou EP, Jarvis ED. Of Mice, Birds, and Men: The Mouse Ultrasonic Song System Has Some Features Similar to Humans and Song-Learning Birds. *PLoS ONE*. 2012; 7(10):e46610. <https://doi.org/10.1371/journal.pone.0046610>. [PubMed: 23071596]
- Atit RP, Mitchell K, Nguyen L, Warshawsky D, Ratner N. The neurofibromatosis type 1 (Nf1) tumor suppressor is a modifier of carcinogen-induced pigmentation and papilloma formation in C57BL/6 mice. *The Journal of Investigative Dermatology*. 2000; 114(6):1093–1100. <https://doi.org/10.1046/j.1523-1747.2000.00994.x>. [PubMed: 10844550]
- Bader PL, Faizi M, Kim LH, Owen SF, Tadross MR, Alfa RW, ... Shamloo M. Mouse model of Timothy syndrome recapitulates triad of autistic traits. *Proceedings of the National Academy of Sciences of the United States of America*. 2011; 108(37):15432–15437. <https://doi.org/10.1073/pnas.1112667108>. [PubMed: 21878566]
- Bajenaru ML, Hernandez MR, Perry A, Zhu Y, Parada LF, Garbow JR, Gutmann DH. Optic Nerve Glioma in Mice Requires Astrocyte Nf1 Gene Inactivation and Nf1 Brain Heterozygosity. *Cancer Research*. 2003; 63(24):8573–8577. Retrieved from <http://cancerres.aacrjournals.org/content/63/24/8573>. [PubMed: 14695164]
- Bajenaru ML, Zhu Y, Hedrick NM, Donahoe J, Parada LF, Gutmann DH. Astrocyte-specific inactivation of the neurofibromatosis 1 gene (NF1) is insufficient for astrocytoma formation. *Molecular and Cellular Biology*. 2002; 22(14):5100–5113. [PubMed: 12077339]
- Barron VA, Lou H. Alternative splicing of the neurofibromatosis type I pre-mRNA. *Bioscience Reports*. 2012; 32(2):131–138. <https://doi.org/10.1042/BSR20110060>. [PubMed: 22115364]
- Branchi I, Santucci D, Alleva E. Ultrasonic vocalisation emitted by infant rodents: a tool for assessment of neurobehavioural development. *Behavioural Brain Research*. 2001; 125(1–2):49–56. [https://doi.org/10.1016/S0166-4328\(01\)00277-7](https://doi.org/10.1016/S0166-4328(01)00277-7). [PubMed: 11682093]
- Branchi I, Santucci D, Vitale A, Alleva E. Ultrasonic vocalizations by infant laboratory mice: a preliminary spectrographic characterization under different conditions. *Developmental Psychobiology*. 1998; 33(3):249–256. [PubMed: 9810475]
- Brannan CI, Perkins AS, Vogel KS, Ratner N, Nordlund ML, Reid SW, ... Copeland NG. Targeted disruption of the neurofibromatosis type-1 gene leads to developmental abnormalities in heart and various neural crest-derived tissues. *Genes & Development*. 1994; 8(9):1019–1029. <https://doi.org/10.1101/gad.8.9.1019>. [PubMed: 7926784]
- Brown JA, Emmett RJ, White CR, Yuede CM, Conyers SB, O'Malley KL, ... Gutmann DH. Reduced striatal dopamine underlies the attention system dysfunction in neurofibromatosis-1 mutant mice. *Human Molecular Genetics*. 2010; 19(22):4515–28. [PubMed: 20826448]
- Cawthon RM, Weiss R, Xu GF, Viskochil D, Culver M, Stevens J, ... O'Connell P. A major segment of the neurofibromatosis type 1 gene: cDNA sequence, genomic structure, and point mutations. *Cell*. 1990; 62(1):193–201. [PubMed: 2114220]

- Cichowski K, Jacks T. NF1 Tumor Suppressor Gene Function. *Cell*. 2001; 104(4):593–604. [https://doi.org/10.1016/S0092-8674\(01\)00245-8](https://doi.org/10.1016/S0092-8674(01)00245-8). [PubMed: 11239415]
- Cichowski K, Shih TS, Schmitt E, Santiago S, Reilly K, McLaughlin ME, ... Jacks T. Mouse models of tumor development in neurofibromatosis type 1. *Science (New York, NY)*. 1999; 286(5447):2172–2176.
- Costa RM, Federov NB, Kogan JH, Murphy GG, Stern J, Ohno M, ... Silva AJ. Mechanism for the learning deficits in a mouse model of neurofibromatosis type 1. *Nature*. 2002; 415(6871):526–530. <https://doi.org/10.1038/nature711>. [PubMed: 11793011]
- D'Amato FR, Scalera E, Sarli C, Moles A. Pups call, mothers rush: does maternal responsiveness affect the amount of ultrasonic vocalizations in mouse pups? *Behavior Genetics*. 2005; 35(1):103–112. <https://doi.org/10.1007/s10519-004-0860-9>. [PubMed: 15674537]
- Dearborn JT, Harmon SK, Fowler SC, O'Malley KL, Taylor GT, Sands MS, Wozniak DF. Comprehensive functional characterization of murine infantile Batten disease including Parkinson-like behavior and dopaminergic markers. *Scientific Reports*. 2015; 5:12752. <https://doi.org/10.1038/srep12752>. [PubMed: 26238334]
- De Filippis B, Ricceri L, Laviola G. Early postnatal behavioral changes in the Mecp2-308 truncation mouse model of Rett syndrome. *Genes, Brain, and Behavior*. 2010; 9(2):213–223. <https://doi.org/10.1111/j.1601-183X.2009.00551.x>.
- D'Gama AM, Pochareddy S, Li M, Jamuar SS, Reiff RE, Lam ATN, ... Walsh CA. Targeted DNA Sequencing from Autism Spectrum Disorder Brains Implicates Multiple Genetic Mechanisms. *Neuron*. 2015; 88(5):910–917. <https://doi.org/10.1016/j.neuron.2015.11.009>. [PubMed: 26637798]
- Diggs-Andrews KA, Brown JA, Gianino SM, Rubin JB, Wozniak DF, Gutmann DH. Sex Is a major determinant of neuronal dysfunction in neurofibromatosis type 1. *Annals of Neurology*. 2014; 75(2):309–316. <https://doi.org/10.1002/ana.24093>. [PubMed: 24375753]
- Diggs-Andrews KA, Tokuda K, Izumi Y, Zorumski CF, Wozniak DF, Gutmann DH. Dopamine deficiency underlies learning deficits in Neurofibromatosis-1 mice. *Annals of Neurology*. 2013; 73(2):309–315. <https://doi.org/10.1002/ana.23793>. [PubMed: 23225063]
- Dougherty JD, Maloney SE, Wozniak DF, Rieger MA, Sonnenblick L, Coppola G, ... Heintz N. The disruption of Celf6, a gene identified by translational profiling of serotonergic neurons, results in autism-related behaviors. *Journal of Neuroscience*. 2013; 33(7):2732–53. [PubMed: 23407934]
- Ehret G. Left hemisphere advantage in the mouse brain for recognizing ultrasonic communication calls. *Nature*. 1987; 325(6101):249–251. <https://doi.org/10.1038/325249a0>. [PubMed: 3808021]
- Ehret G. Categorical perception of mouse-pup ultrasounds in the temporal domain. *Animal Behaviour*. 1992; 43(3):409–416. [https://doi.org/10.1016/S0003-3472\(05\)80101-0](https://doi.org/10.1016/S0003-3472(05)80101-0).
- Ehret G, Haack B. Ultrasound recognition in house mice: Key-Stimulus configuration and recognition mechanism. *Journal of Comparative Physiology*. 1982; 148(2):245–251. <https://doi.org/10.1007/BF00619131>.
- Faul F, Erdfelder E, Lang AG, Buchner A. G*Power 3: A flexible statistical power analysis program for the social, behavioral, and biomedical sciences. *Behavior Research Methods*. 2007; 39:175–191. [PubMed: 17695343]
- Garg S, Green J, Leadbitter K, Emsley R, Lehtonen A, Evans DG, Huson SM. Neurofibromatosis Type 1 and Autism Spectrum Disorder. *Pediatrics*. 2013; 132(6):e1642–e1648. <https://doi.org/10.1542/peds.2013-1868>. [PubMed: 24190681]
- Garg S, Lehtonen A, Huson SM, Emsley R, Trump D, Evans DG, Green J. Autism and other psychiatric comorbidity in neurofibromatosis type 1: evidence from a population-based study. *Developmental Medicine and Child Neurology*. 2013; 55(2):139–145. <https://doi.org/10.1111/dmcn.12043>. [PubMed: 23163236]
- Gutmann DH. Neurofibromin in the brain. *Journal of Child Neurology*. 2002; 17(8):592–601. discussion 602–604, 646–651. [PubMed: 12403558]
- Gutmann DH, Giovannini M. Mouse Models of Neurofibromatosis 1 and 2. *Neoplasia (New York, NY)*. 2002; 4(4):279–290. Retrieved from <http://www.ncbi.nlm.nih.gov/pmc/articles/PMC1531708/>.
- Gutmann DH, McLellan MD, Hussain I, Wallis JW, Fulton LL, Fulton RS, ... Mardis ER. Somatic neurofibromatosis type 1 (NF1) inactivation characterizes NF1-associated pilocytic astrocytoma.

- Genome Research. 2013; 23(3):431–439. <https://doi.org/10.1101/gr.142604.112>. [PubMed: 23222849]
- Haack, B., Markl, H., Ehret, G. The Comparative Psychology of Audition: Perceiving Complex Sounds. Psychology Press; 1983. Sound communication between parents and offspring. Retrieved from <https://oparu.uni-ulm.de/xmlui/handle/123456789/1201>
- Hahn ME, Lavooy MJ. A review of the methods of studies on infant ultrasound production and maternal retrieval in small rodents. Behavior Genetics. 2005; 35(1):31–52. <https://doi.org/10.1007/s10519-004-0854-7>. [PubMed: 15674531]
- Hofer, MA., Shair, HN., Brunelli, SA. Current Protocols in Neuroscience. John Wiley & Sons, Inc; 2002. Ultrasonic Vocalizations in Rat and Mouse Pups. Retrieved from <http://onlinelibrary.wiley.com/doi/10.1002/0471142301.ns0814s17/abstract>
- Holy TE, Guo Z. Ultrasonic Songs of Male Mice. PLoS Biol. 2005; 3(12):e386. <https://doi.org/10.1371/journal.pbio.0030386>. [PubMed: 16248680]
- Hyman SL, Shores A, North KN. The nature and frequency of cognitive deficits in children with neurofibromatosis type 1. Neurology. 2005; 65(7):1037–1044. <https://doi.org/10.1212/01.wnl.0000179303.72345.ce>. [PubMed: 16217056]
- Jacks T, Shih TS, Schmitt EM, Bronson RT, Bernards A, Weinberg RA. Tumour predisposition in mice heterozygous for a targeted mutation in Nf1. Nature Genetics. 1994; 7(3):353–361. <https://doi.org/10.1038/ng0794-353>. [PubMed: 7920653]
- Jamuar SS, Lam ATN, Kircher M, D’Gama AM, Wang J, Barry BJ, ... Walsh CA. Somatic mutations in cerebral cortical malformations. The New England Journal of Medicine. 2014; 371(8):733–743. <https://doi.org/10.1056/NEJMoa1314432>. [PubMed: 25140959]
- Jett K, Friedman JM. Clinical and genetic aspects of neurofibromatosis 1. Genetics in Medicine. 2010; 12(1):1–11. <https://doi.org/10.1097/GIM.0b013e3181bf15e3>. [PubMed: 20027112]
- Jouhilahti EM, Peltonen S, Heape AM, Peltonen J. The Pathoetiology of Neurofibromatosis 1. The American Journal of Pathology. 2011; 178(5):1932–1939. <https://doi.org/10.1016/j.ajpath.2010.12.056>. [PubMed: 21457932]
- Krömer SA, Keßler MS, Milfay D, Birg IN, Bunck M, Czibere L, ... Turck CW. Identification of Glyoxalase-I as a Protein Marker in a Mouse Model of Extremes in Trait Anxiety. Journal of Neuroscience. 2005; 25(17):4375–4384. <https://doi.org/10.1523/JNEUROSCI.0115-05.2005>. [PubMed: 15858064]
- Lai JKY, Sobala-Drozdowski M, Zhou L, Doering LC, Faure PA, Foster JA. Temporal and spectral differences in the ultrasonic vocalizations of fragile X knock out mice during postnatal development. Behavioural Brain Research. 2014; 259:119–130. <https://doi.org/10.1016/j.bbr.2013.10.049>. [PubMed: 24211451]
- Michetti, C., Ricceri, L., Scattoni, ML. Modeling Social Communication Deficits in Mouse Models of Autism; Autism-Open Access. 2012. p. 2-8. <https://doi.org/10.4172/2165-7890.S1-007>
- Molosh AI, Johnson PL, Spence JP, Arendt D, Federici LM, Bernabe C, ... Shekhar A. Social learning and amygdala disruptions in Nf1 mice are rescued by blocking p21-activated kinase. Nature Neuroscience. 2014; 17(11):1583–1590. <https://doi.org/10.1038/nn.3822>. [PubMed: 25242307]
- Morris SM, Acosta MT, Garg S, Green J, Huson S, Legius E, ... Constantino JN. Disease Burden and Symptom Structure of Autism in Neurofibromatosis Type 1: A Study of the International NF1-ASD Consortium Team (INFACT). JAMA Psychiatry. 2016; 73(12):1276–1284. <https://doi.org/10.1001/jamapsychiatry.2016.2600>. [PubMed: 27760236]
- Moy SS, Nadler JJ, Magnuson TR, Crawley JN. Mouse models of autism spectrum disorders: the challenge for behavioral genetics. American Journal of Medical Genetics. Part C, Seminars in Medical Genetics. 2006; 142C(1):40–51. <https://doi.org/10.1002/ajmg.c.30081>.
- Petrella LI, Cai Y, Sereno JV, Gonçalves SI, Silva AJ, Castelo-Branco M. Brain and behaviour phenotyping of a mouse model of neurofibromatosis type-1: an MRI/DTI study on social cognition. Genes, Brain and Behavior. 2016; 15(7):637–646. <https://doi.org/10.1111/gbb.12305>.
- Rieger MA, Dougherty JD. Analysis of within Subjects Variability in Mouse Ultrasonic Vocalization: Pups Exhibit Inconsistent, State-Like Patterns of Call Production. Frontiers in Behavioral Neuroscience. 2016; 10 <https://doi.org/10.3389/fnbeh.2016.00182>.

- Scattoni ML, Gandhi SU, Ricceri L, Crawley JN. Unusual Repertoire of Vocalizations in the BTBR T +tf/J Mouse Model of Autism. *PLOS ONE*. 2008; 3(8):e3067. <https://doi.org/10.1371/journal.pone.0003067>. [PubMed: 18728777]
- Sewell GD. Ultrasonic communication in rodents. *Nature*. 1970; 227(5256):410.
- Silva AJ, Frankland PW, Marowitz Z, Friedman E, Lazlo G, Cioffi D, ... Bourtchuladze R. A mouse model for the learning and memory deficits associated with neurofibromatosis type I. *Nature Genetics*. 1997; 15(3):281–284. <https://doi.org/10.1038/ng0397-281>. [PubMed: 9054942]
- Smith JC. Responses of adult mice to models of infant calls. *Journal of Comparative and Physiological Psychology*. 1976; 90(12):1105–1115. <https://doi.org/10.1037/h0077287>.
- Spyk SL, Thomas N, Cooper DN, Upadhyaya M. Neurofibromatosis type 1-associated tumours: Their somatic mutational spectrum and pathogenesis. *Human Genomics*. 2011; 5:623. <https://doi.org/10.1186/1479-7364-5-6-623>. [PubMed: 22155606]
- Szudek J, Birch P, Riccardi Vm, Evans Dg, Friedman Jm. Associations of clinical features in neurofibromatosis 1 (NF1). *Genetic Epidemiology*. 2000; 19(4):429–439. [https://doi.org/10.1002/1098-2272\(200012\)19:4<429::AID-GEPI13>3.0.CO;2-N](https://doi.org/10.1002/1098-2272(200012)19:4<429::AID-GEPI13>3.0.CO;2-N). [PubMed: 11108651]
- van Velzen A, Toth M. Role of maternal 5-HT1A receptor in programming offspring emotional and physical development. *Genes, Brain, and Behavior*. 2010; 9(8):877–885. <https://doi.org/10.1111/j.1601-183X.2010.00625.x>.
- Walsh KS, Vélez JI, Kardel PG, Imas DM, Muenke M, Packer RJ, ... Acosta MT. Symptomatology of autism spectrum disorder in a population with neurofibromatosis type 1. *Developmental Medicine and Child Neurology*. 2013; 55(2):131–138. <https://doi.org/10.1111/dmcn.12038>. [PubMed: 23163951]
- Weiss JB, Weber SJ, Torres ERS, Marzulla T, Raber J. Genetic inhibition of Anaplastic Lymphoma Kinase rescues cognitive impairments in Neurofibromatosis 1 mutant mice. *Behavioural Brain Research*. 2017; 321:148–156. <https://doi.org/10.1016/j.bbr.2017.01.003>. [PubMed: 28057529]
- Weiss, JB., Weber, S., Marzulla, T., Raber, J. Pharmacological inhibition of Anaplastic Lymphoma Kinase rescues spatial memory impairments in Neurofibromatosis 1 mutant mice. *Behavioural Brain Research*. n.d. <https://doi.org/10.1016/j.bbr.2017.06.024>
- Weller A, Leguisamo AC, Towns L, Ramboz S, Bagiella E, Hofer M, ... Brunner D. Maternal effects in infant and adult phenotypes of 5HT1A and 5HT1B receptor knockout mice. *Developmental Psychobiology*. 2003; 42(2):194–205. <https://doi.org/10.1002/dev.10079>. [PubMed: 12555283]
- Wöhr M. Ultrasonic vocalizations in Shank mouse models for autism spectrum disorders: Detailed spectrographic analyses and developmental profiles. *Neuroscience & Biobehavioral Reviews*. 2014; 43:199–212. <https://doi.org/10.1016/j.neubiorev.2014.03.021>. [PubMed: 24726578]
- Wöhr M, Dahlhoff M, Wolf E, Holsboer F, Schwarting RKW, Wotjak CT. Effects of Genetic Background, Gender, and Early Environmental Factors on Isolation-Induced Ultrasonic Calling in Mouse Pups: An Embryo-Transfer Study. *Behavior Genetics*. 2008; 38(6):579–595. <https://doi.org/10.1007/s10519-008-9221-4>. [PubMed: 18712592]
- Wöhr M, van Gaalen MM, Schwarting RKW. Affective communication in rodents: serotonin and its modulating role in ultrasonic vocalizations. *Behavioural Pharmacology*. 2015; 26(6):506–521. <https://doi.org/10.1097/FBP.0000000000000172>. [PubMed: 26221830]
- Wozniak DF, Diggs-Andrews KA, Conyers S, Yuede CM, Dearborn JT, Brown JA, ... Gutmann DH. Motivational Disturbances and Effects of L-dopa Administration in Neurofibromatosis-1 Model Mice. *PLOS ONE*. 2013; 8(6):e66024. <https://doi.org/10.1371/journal.pone.0066024>. [PubMed: 23762458]
- Young DM, Schenk AK, Yang SB, Jan YN, Jan LY. Altered ultrasonic vocalizations in a tuberous sclerosis mouse model of autism. *Proceedings of the National Academy of Sciences*. 2010; 107(24):11074–11079. <https://doi.org/10.1073/pnas.1005620107>.
- Zhu Y, Ghosh P, Charnay P, Burns DK, Parada LF. Neurofibromas in NF1: Schwann Cell Origin and Role of Tumor Environment. *Science (New York, NY)*. 2002; 296(5569):920–922. <https://doi.org/10.1126/science.1068452>.
- Zhu Y, Romero MI, Ghosh P, Ye Z, Charnay P, Rushing EJ, ... Parada LF. Ablation of NF1 function in neurons induces abnormal development of cerebral cortex and reactive gliosis in the brain. *Genes & Development*. 2001; 15(7):859–876. <https://doi.org/10.1101/gad.862101>. [PubMed: 11297510]

Lay Summary

Neurofibromatosis type 1 (NF1) is a common neurogenetic disorder caused by mutation of the *NF1* gene, in which 80% of affected children exhibit cognitive and behavioral issues. Based on emerging evidence that NF1 may be an autism predisposition gene, we examined ASD-relevant early communicative behavior in *Nf1* mouse models and observed alterations in both models. The changes in early communicative behavior in *Nf1* mutant mice should motivate further studies into the causative factors and potential treatments for ASD arising in the context of NF1.

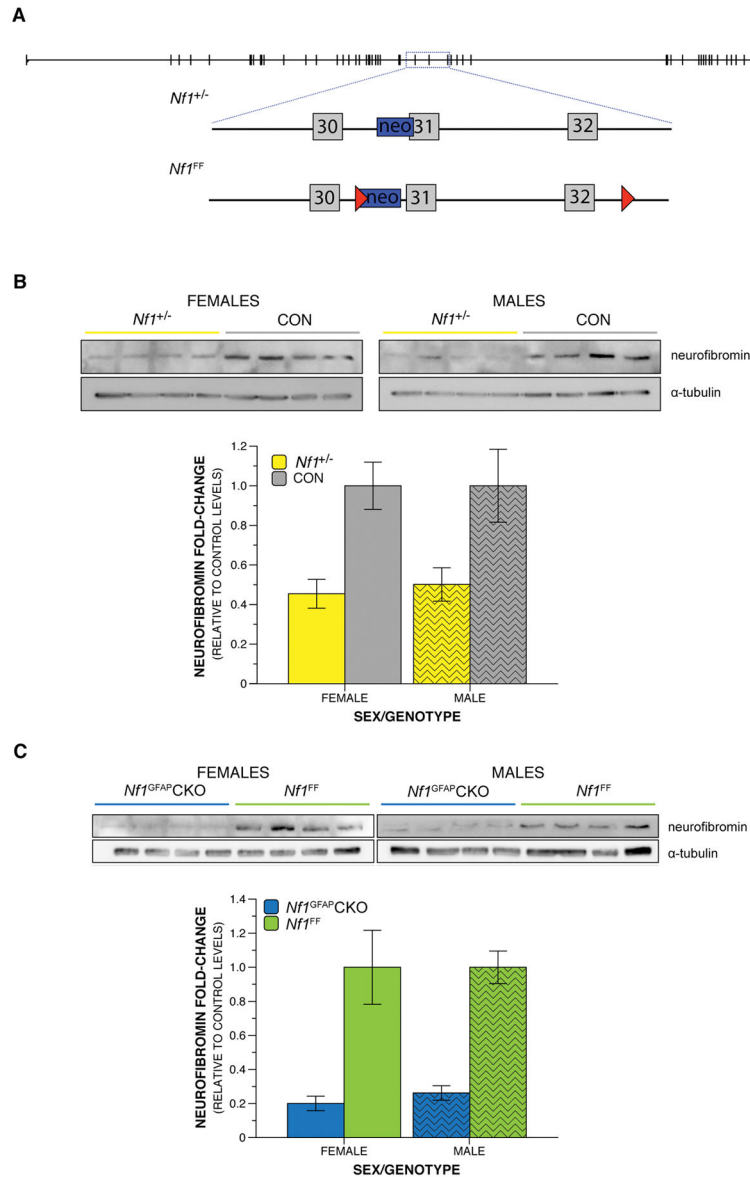


Figure 1. *Nf1* germline heterozygosity and somatic biallelic inactivation differentially decrease neurofibromin levels

A) Distinct targeted disruptions of the *Nf1* gene locus in the mouse are shown by a schematic of the murine *Nf1* gene, represented by the black line with exons depicted as intersecting narrow rectangles. The area within the blue dashed box is enlarged to show details of specific genetic alterations. Gray boxes represent exons, blue boxes represent a neomycin cassette, and the red triangles show loxP sites. The *Nf1*^{+/-} loss-of-function mutation results from an insertion of a neomycin cassette within a portion of intron 30 (38) and exon 31 (39). The *Nf1*^{FF} mice contain a loxP site attached to a neomycin cassette within intron 30 (38) and a second loxP site within intron 32 (40). **B–C)** Representative western blot images and quantification. **B)** Neurofibromin levels were reduced in the brains of P21 *Nf1*^{+/-} mice compared to control littermates by 55% in females and 50% in males. **C)**

Neurofibromin levels were reduced in the brains of P21 male and female *Nf1*^{GFAP}CKO mice compared to control littermates by 80% in females and 74% in males.

Author Manuscript

Author Manuscript

Author Manuscript

Author Manuscript

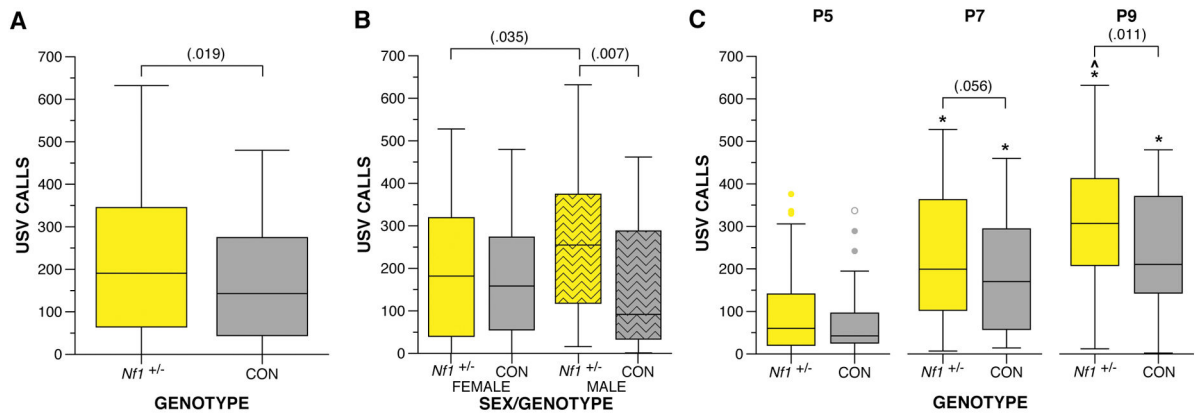


Figure 2. Germline heterozygous mutation in the *Nf1* gene results in increased USV production when separated from dam during development

Nf1^{+/-} and control littermates were evaluated for USV production during the first two weeks postnatal. **A)** *Nf1*^{+/-} mice produce significantly more USV calls during development compared to control littermates, $F(1,68) = 5.737$, $p = .019$. **B)** Male *Nf1*^{+/-} mice exhibit more USV calls compared to male controls, $F(1,68) = 7.669$, $p = .007$, and female *Nf1*^{+/-} mice, $F(1,68) = 4.611$, $p = .035$. **C)** *Nf1*^{+/-} mutants produced marginally more USVs on P7 compared to controls, $F(1,204) = 3.691$, $p = .056$, and significantly more USVs compared to controls, $F(1,204) = 6.570$, $p = .011$. Control mice increased USV calls only from P5 to P7 ($p < .05$, 95% CI [48.59, 158.58]), while *Nf1*^{+/-} mice showed a further increase by P9 (P7 $p < .05$, 95% CI [88.45, 202.23], P9 $p < .05$, 95% CI [-6.865, 137.44]). Boxplots represent number of USV calls at P5, P7, and P9. *indicates significant differences from P5 ($p < .05$). ^indicates a marginal significant difference from P7 ($p < .1$). Thick horizontal lines signify respective group medians, boxes are 25th – 75th percentiles, whiskers are 1.5 x IQR, closed and open circles depict outliers.

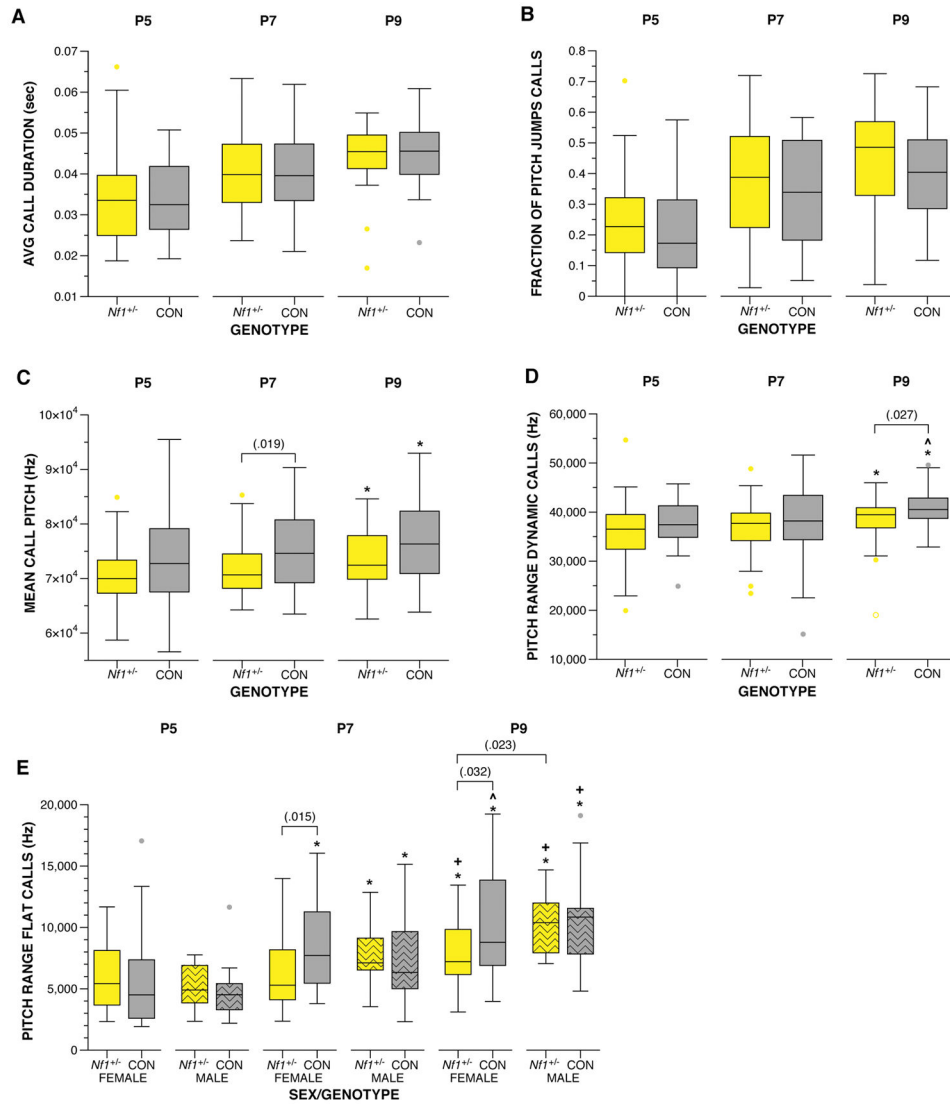


Figure 3. Examination of the spectral features of the *Nf1*^{+/-} USVs revealed alterations in pitch
A) USV calls from both *Nf1*^{+/-} and controls were similar in duration and **B)** fraction of calls containing a pitch jump. **C)** The mean pitch frequency of *Nf1*^{+/-} USVs was lower compared to controls, $F(1,67.833) = 5.429$, $p = .023$, with the greatest difference observed at P7, $F(1,150.915) = 5.647$, $p = .019$. **D)** *Nf1*^{+/-} USVs exhibited a narrower range of pitch compared to controls, $F(1,168.563) = 5.675$, $p = .018$, particularly at P9, $F(1,65) = 5.096$, $p = .027$. **E)** A narrower pitch range was also observed for female *Nf1*^{+/-} flat calls at P7, $F(1,116.846) = 6.158$, $p = .015$ and P9, $F(1,115.322) = 4.692$, $p = .032$, compared to female controls, and male *Nf1*^{+/-} mice at P9, $F(1,115.322) = 5.276$, $p = .023$. All animals increased average pitch and range with age. *indicates differences from P5 ($p < .05$). + indicates a difference from P7 ($p < .05$). ^ indicates a marginal difference from P7 ($p < .1$). Thick horizontal lines signify respective group medians, boxes are 25th – 75th percentiles, whiskers are 1.5xIQR, closed and open circles depict outliers.

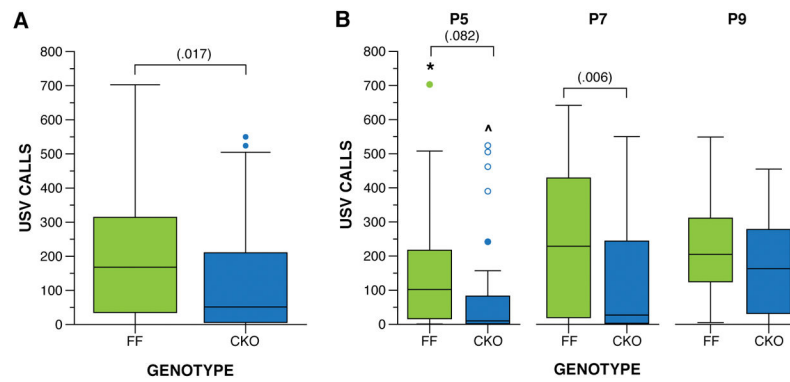


Figure 4. Biallelic deletion of *Nfl* gene in neuroglial precursor cells results in reduced USVs in pups

Nfl^{FF} and *Nfl*^{GFAP}CKO littermates were evaluated for USVs during the first two weeks postnatal. **A)** *Nfl*^{GFAP}CKO produced significantly less USV calls during development compared to their control littermates, $F(1,71) = 5.963$, $p = .017$. **B)** The greatest difference in USVs occurred on P7, $F(1,213) = 7.660$, $p = .006$. All mice significantly increased USVs with age, $F(2,142) = 8.742$, $p = .000$. Within each genotype, control mice showed an increase in USVs, $F(2,70) = 5.670$, $p = .005$, from P5 to P7 ($p < .05$) and P9, although the difference from P9 did not reach statistical significance. The *Nfl*^{GFAP}CKO littermates demonstrated an increase in USVs, $F(2,70) = 4.735$, $p = .012$, only from P5 to P9 ($p < .05$). Boxplots represent USV calls when removed from dam at P5, P7, and P9. *indicates difference from P7 ($p < .05$), ^ indicates difference from P9 ($p < .05$). Thick horizontal lines signify respective group medians, boxes are 25th – 75th percentiles, whiskers are 1.5 x IQR, closed and open circles depict outliers.

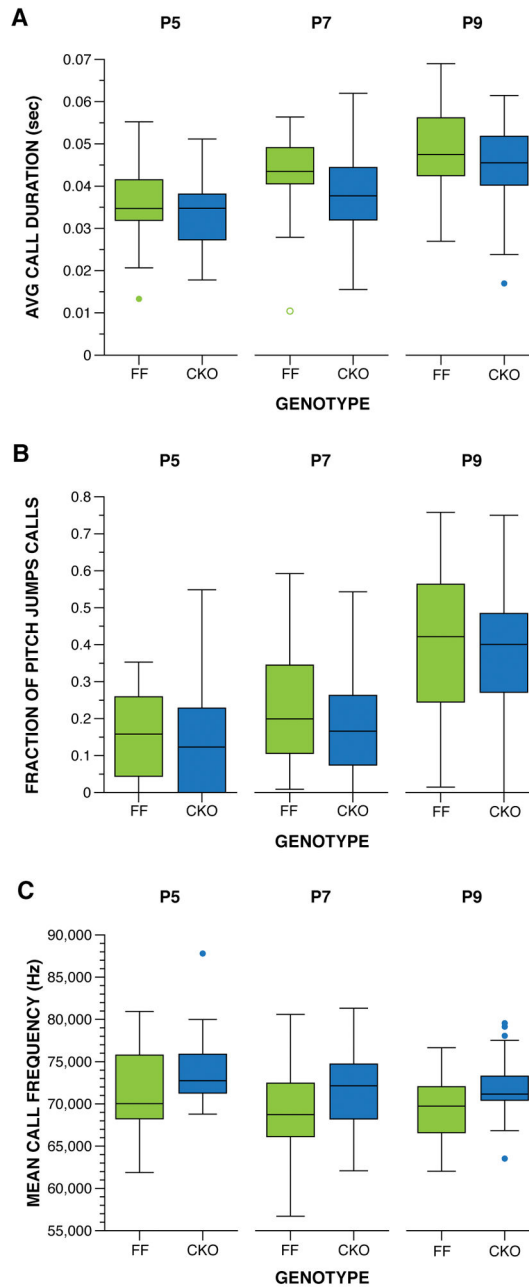


Figure 5. Spectral features of the USVs were unchanged by biallelic inactivation of *Nfl*
A) USV calls from both *Nfl*^{GFAP}CKO and *Nfl*^{FF} littermates were on average the similar in duration. **B)** Both *Nfl*^{GFAP}CKO and *Nfl*^{FF} littermates produced a similar fraction of calls containing a pitch jump. **C)** The mean frequency of the USV calls produced was comparable for all mice. Boxplots represent **(A)** average duration, **(B)** fraction of calls containing a pitch jump, and **(C)** mean frequency of USV calls produced on P5, P7 and P9. Thick horizontal lines signify respective group medians, boxes are 25th – 75th percentiles, whiskers are 1.5 x IQR, closed and open circles depict outliers.

Table 1

Sample sizes distributed between sexes.

Animal Line	Males	Females	Total	Litters
<i>Nf1^{+/-}</i>	13	23	36	14
<i>Nf1^{+/+}</i> controls	16	20	36	
<i>Nf1^{GFAP}CKO</i>	19	19	38	10
<i>Nf1^{FF}</i> controls	16	19	35	

Author Manuscript

Author Manuscript

Author Manuscript

Author Manuscript

Table 2

Percent of somatic biallelic deletion mice producing < 10 calls per session.

Age	<i>Nf1</i> ^{GFAPCKO}	<i>Nf1</i> ^{FF} controls	Fisher's Exact <i>p</i> value
P5	50%	20%	.007
P7	37%	20%	.091
P9	16%	3%	.067

Author Manuscript

Author Manuscript

Author Manuscript

Author Manuscript

Table 3

Dopamine, DOPAC, HVA, serotonin, and 5-HIAA levels in whole-brain.

Animal Line	DA (ng/mg)	DOPAC (ng/mg)	HVA (ng/mg)	5-HT (ng/mg)	5-HIAA (ng/mg)
<i>Nf1^{+/-}</i>	0.191 ± 0.010	0.101 ± 0.005	0.085 ± 0.005	0.228 ± 0.007 [*]	0.145 ± 0.008
<i>Nf1^{+/+}</i> controls	0.182 ± 0.008	0.096 ± 0.004	0.078 ± 0.004	0.205 ± 0.002 [*]	0.125 ± 0.007
<i>Nf1^{GFPCKO}</i>	0.195 ± 0.012	0.133 ± 0.004	0.068 ± 0.005	0.204 ± 0.006 [^]	0.158 ± 0.014 [^]
<i>Nf1^{FF}</i> controls	0.204 ± 0.006	0.126 ± 0.002	0.074 ± 0.004	0.191 ± 0.002 [^]	0.129 ± 0.006 [^]

Results are mean ± SEM.

^{*} $p < .05$,

[^] $p < .1$.